Supporting Information

Many Lives of Cobalt within Electrochemical Systems: from Waste Batteries to Efficient Hydrogen Evolution Reaction Electrocatalyst

[1]Lorenzo Mirizzi[+], [1]Eleonora Carena[+], [1]Carlo Santoro, [2,3]Valerio C.A. Ficca, [2]Ernesto Placidi, [3]Enrico Berretti, [4]Alessandro Lavacchi, [1]Chiara Ferrara*, [1]Mohsin Muhyuddin**

1 Department of Materials Science University of Milano-Bicocca, U5, Via Roberto Cozzi 55, 20125, Milan (MI), Italy

[2] Department of Physics, Sapienza University of Rome, Piazzale Aldo Moro 2, 00185 Roma, Italy

[3] TERIN Department, Division of Technologies and Vectors for Decarbonization, ENEA Casaccia Research Center, Via Anguillarese 301, 00123 Santa Maria di Galeria, Rome, Italy

[4] Istituto di Chimica Dei Composti OrganoMetallici (ICCOM), Consiglio Nazionale Delle Ricerche (CNR), Via Madonna Del Piano 10, 50019 Sesto Fiorentino, Firenze (Italy)

+ contributed equally

Corresponding Authors:

*Chiara Ferrara: chiara.ferrara@unimib.it

**Mohsin Muhyuddin: mohsin.muhyuddin@unimib.it

Table S1. Elemental composition

	at.%						
	O1s	**Co2p**	**C1s**	**F1s**	**P2p**	**Li1s**	**Al2s**
c-LCO	55.1	16.9	0.4	0.0	0.0	27.7	0.0
p-LCO-400	55.8	15.0	0.2	0.0	0.0	28.9	0.0
p-LCO-550	87.3	11.5	1.2	0.0	0.0	0.0	0.0
p-LCO-700	78.5	19.8	1.7	0.0	0.0	0.0	0.0
w-LCO	50.6	3.7	2.5	34.0	4.9	0.0	4.3
r-LCO	77.9	20.3	1.8	0.0	0.0	0.0	0.0

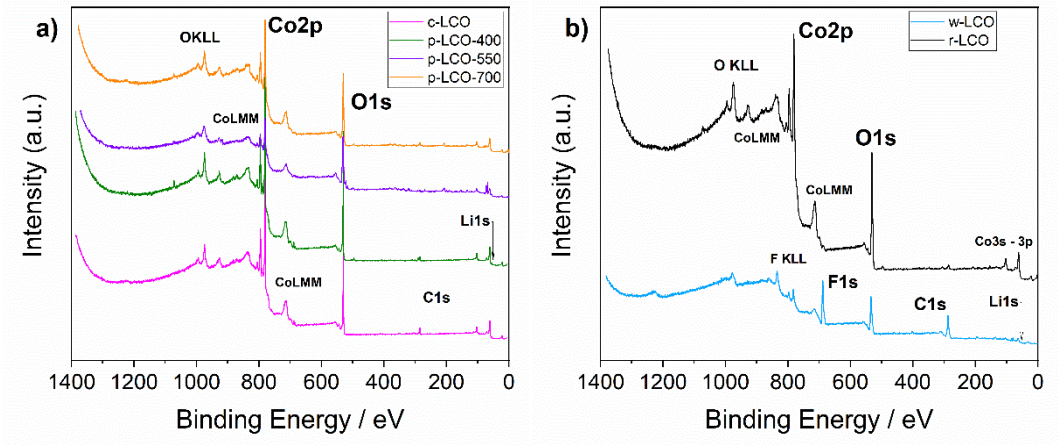

Figure S1. Survey scans of LCO samples showing all the elements identified. a) c-LCO and p-LCO-T, b) w-LCO and r-LCO-based samples.

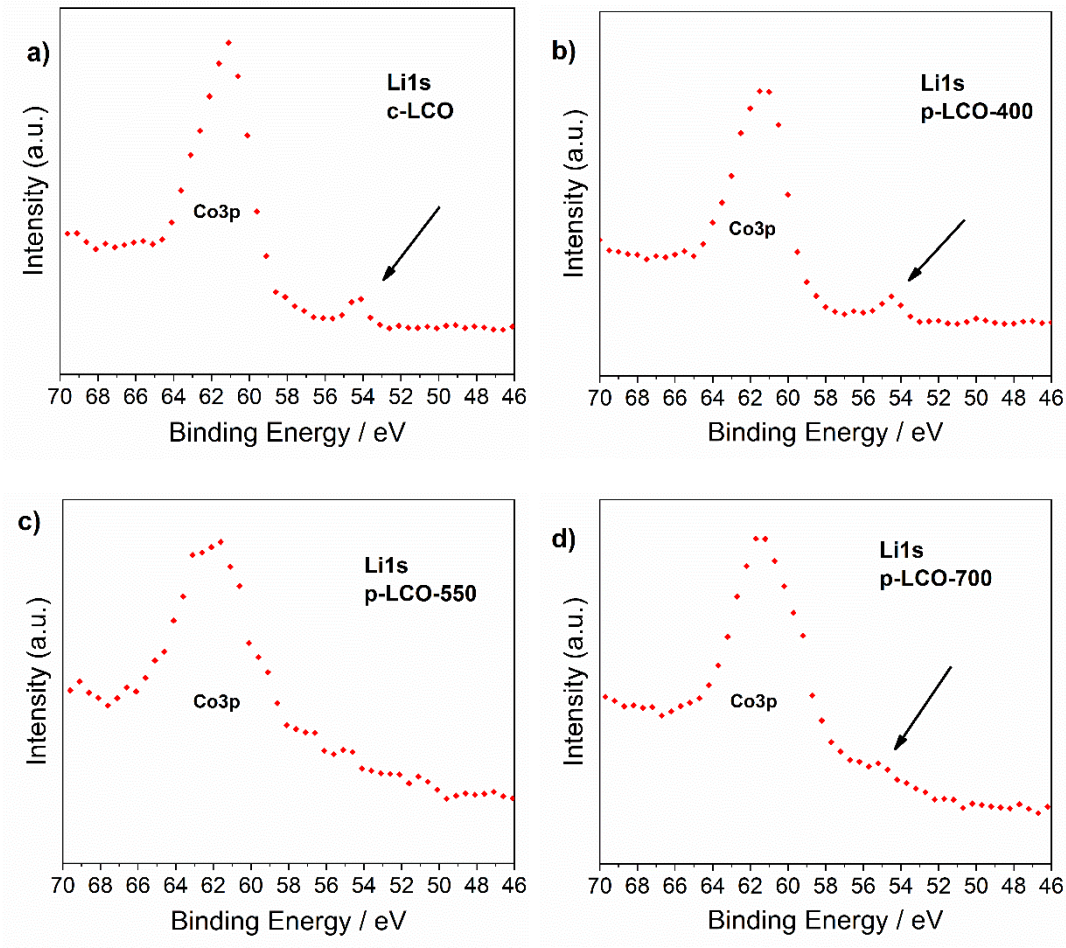

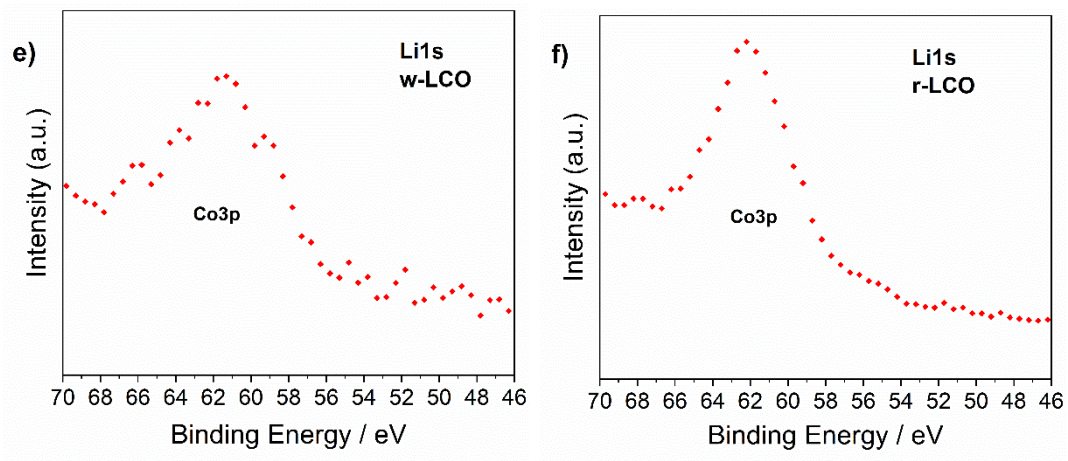

Figure S2. Li1s signal of LCO samples (black arrow). a) c-LCO, b) p-LCO-400, c) p-LCO-550, d) p-LCO-700, e) w-LCO, f) r-LCO. The Co3p peak is also reported and complicates the evaluation of Li1s.

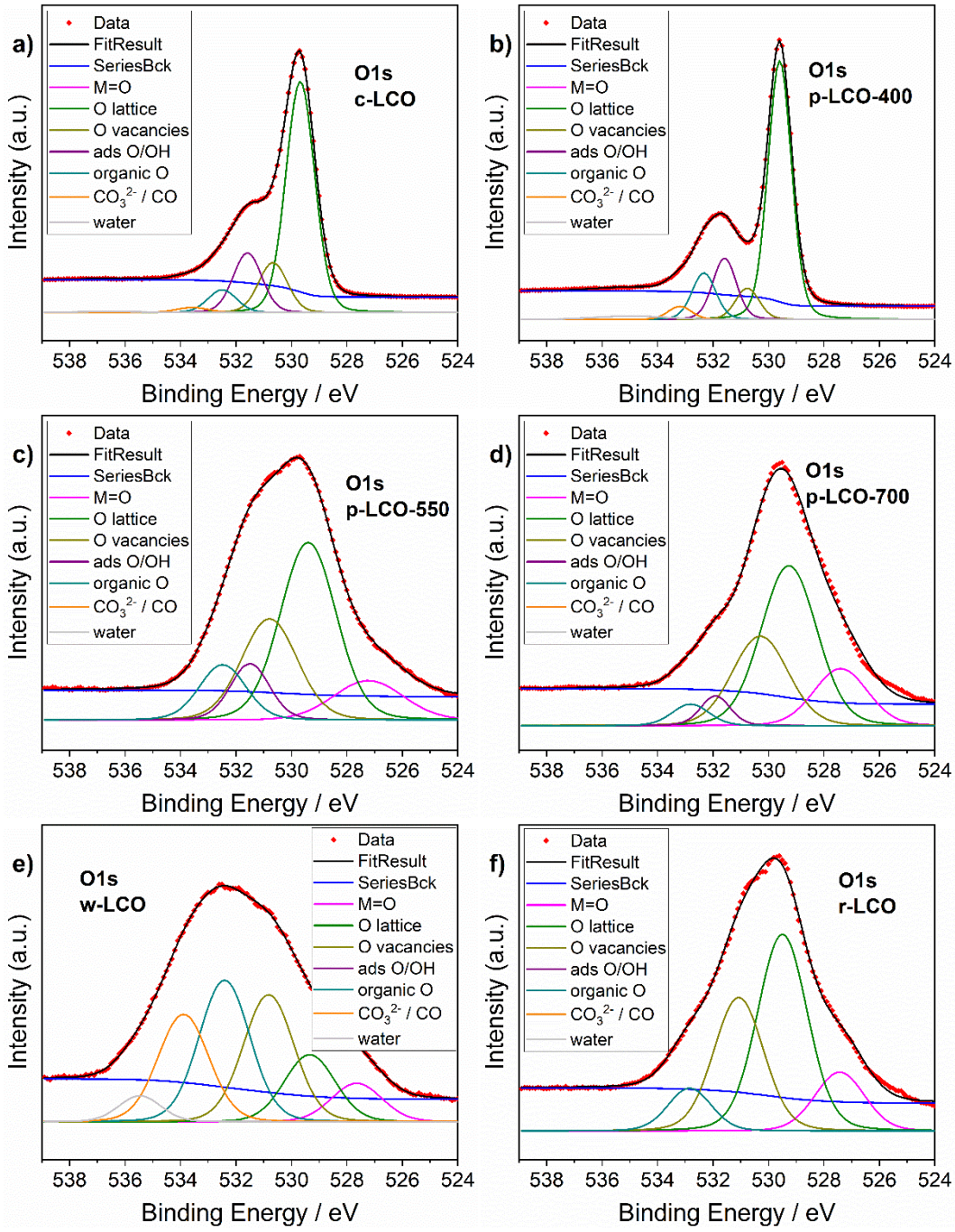

Figure S3. O1s spectra of LCO samples. a) C-LCO, b) P-LCO-400, c) P-LCO-550, d) P-LCO-700, e) W-LCO, f) r-LCO.

Fitting criteria for Co2p and O1s core levels.

The Co2p spectra were deconvoluted into two main components and two characteristic satellites. The Co(III) at 779 - 780 eV and the corresponding satellite at 790 eV, the Co(II) at 780 – 781 eV with its satellite at 785-786 eV. [1–3] An additional peak was also included between 782 – 783 eV according to the literature of Co_3O_4 and ascribed to multiple transitions. [4]The peak was required due to the similarities in terms of the spectra' shape of the samples with that mixed Co compound. C 1s core levels were acquired as well and fitted according to previous studies (data not shown). [5, 6]Within the O1s fitting, seven different components were identified and associated with O double bonded to metal (M=O, < 528 eV), [7]O in the crystalline lattice (O lattice, 528.5 – 529.5 eV), [8] O defects

and vacancies (O vacancies, 530 – 531 eV, [9] surface adsorbed O and OH groups (ads O/OH, 531 – 532 eV), [10]various forms of organic O adsorbed over the surface (organic O, 532 – 533 eV), [11]carbonate and CO groups (CO_3^{2-}/CO, 533 – 534 eV), [12] and adsorbed water (>534 eV). [6]

Table S2. Chemical Speciation of identified elements

	c-LCO		p-LCO-400		p-LCO-550		p-LCO-700		w-LCO		r-LCO	
Comp	**BE (eV)**	**rel. %**	**BE (eV)**	**rel. %**	**BE (eV)**	**rel. %**	**BE (eV)**	**rel. %**	**BE (eV)**	**rel. %**	**BE (eV)**	**rel. %**
M=O					527.2	*11.8*	527.4	*16.5*	527.6	*7.6*	527.4	*13.8*
O lattice	529.7	*62.6*	529.6	*61.4*	529.4	*42.8*	529.3	*47.6*	529.3	*13.3*	529.5	*46.1*
O vacancies	530.7	*13.5*	530.8	*7.4*	530.8	*24.4*	530.3	*26.6*	530.8	*25.2*	531.1	*31.3*
ads O/OH	531.6	*16.2*	531.6	*14.6*	531.5	*9.8*	531.9	*5.0*				
organic O	532.5	*6.2*	532.3	*11.0*	532.5	*11.2*	532.8	*4.4*	532.4	*28.1*	532.8	*8.9*
CO_3^{2-}/CO	533.6	*1.6*	533.2	*3.1*					533.9	*21.3*		
water			535.0	*2.4*					535.5	*4.3*		
Co(III)	780.0	*41.7*	779.9	*46.0*	779.6	*60.1*	779.5	*67.5*	779.5	*38.7*	779.7	*58.4*
Co(II)	781.0	*38.3*	781.0	*35.1*	780.7	*23.9*	780.8	*20.8*	781.1	*40.5*	780.9	*30.5*
multiplet	782.5	*19.9*	782.5	*18.9*	782.9	*15.9*	783.2	*11.7*	782.5	*20.8*	782.8	*11.0*
sat Co(II)	785.1	*0.0*	785.0	*0.0*	785.7	*0.0*	786.0	*0.0*	785.7	*0.0*	785.6	*0.0*
sat Co(III)	790.0	*0.0*	789.9	*0.0*	790.2	*0.0*	790.2	*0.0*	790.2	*0.0*	790.5	*0.0*
C defect									284.0	*24.3*		
C-C/C-H	285.0	*66.9*	285.2	*37.8*			285.0	*100.0*				
C-OH/C-O-C	286.3	*16.7*	286.6	*11.7*	286.1	*100.0*			286.5	*61.9*	286.0	*100.0*
C=O	288.6	*10.5*	288.7	*18.5*					289.9	*13.8*		
O-C=O/O=C-OH	290.3	*5.9*	290.3	*32.0*								
Shake-up	292.9	*0.0*	291.2	*0.0*								

F1									687.4	*82.2*		
F2									684.8	*17.8*		
P1									132.9	*33.4*		
P2									136.1	*66.6*		
Li1s												
Al									120.9	*100.0*		

The electrochemical analysis was commenced with the acquisition of cyclic voltammograms (CVs) in the working electrolyte of 1M KOH and the achieved trends have been displayed in Figure S4. When the glassy carbon electrode was deposited with the electrocatalytic samples i.e. p-LCO-700 and r-LCO in their pristine form several redox peaks appeared in the positive window whose intensities were further enhanced when the sample r-LCO was mixed with KJB and Vulcan XC72R in 20/80 ratio and the corresponding samples i.e K-r-LCO and V-r-LCO inferred to be relatively more redox active. However, the electrochemical redox events above 0 V vs RHE remain beyond the scope of the presented study. Nevertheless, it's important to highlight that beyond such redox events (particularly below ca. -0.2 V vs RHE) the HER initiated. Comparatively earlier onset of HER of r-LCO was further improved with the addition of carbons i.e. KJB and Vulcan XC72R, enhancing the HER rates as indicated by the sharper peaks.

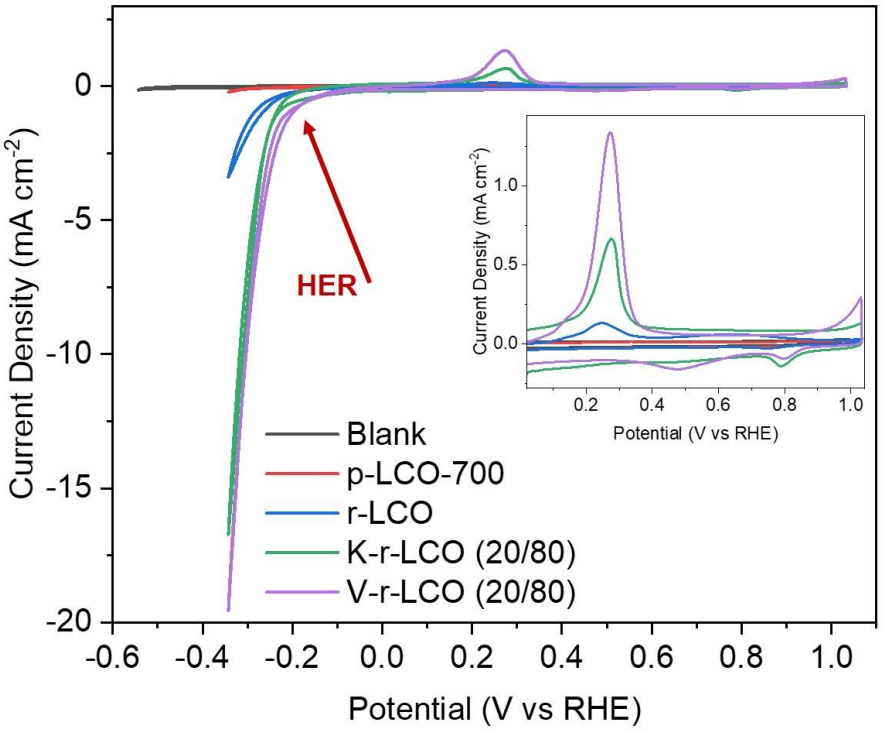

Figure S4: Cyclic Voltammetry (CV) run without any sample on the electrode surface (Blank) and with the deposited (0.6 mg cm^{-2}) on the glassy carbon electrode in the N_2-saturated 1M KOH under stationary conditions at 5mV s^{-1} scan rate. CV was performed on the p-LCO-700 and r-LCO in pure form while the sample r-LCO with the 80 wt.% addition of KJB (K-r-LCO) and Vulcan XC72R (V-r-LCO) was analyzed separately.

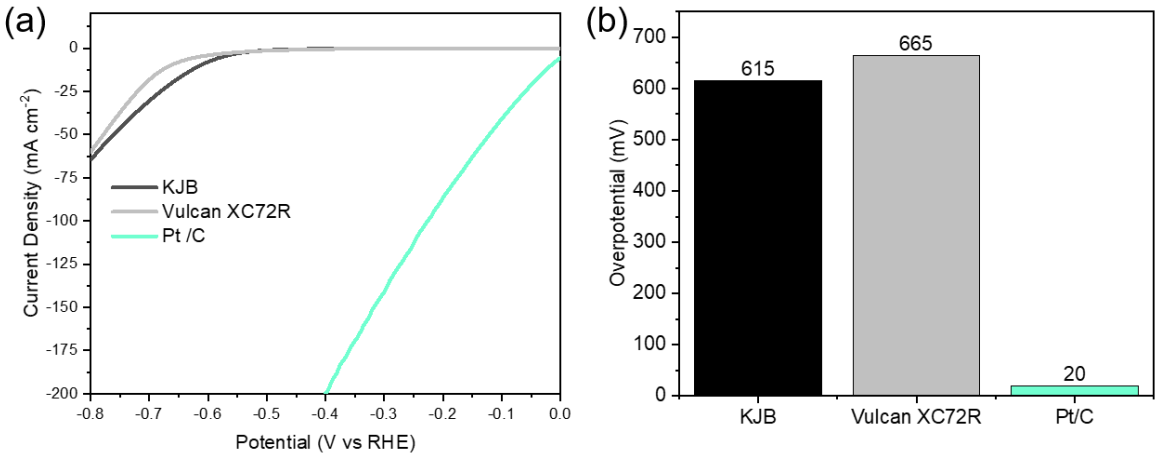

Figure S5: HER activities of pure carbon black i.e. KJB and VulcanXC72R, and benchmark Pt/C (containing 40 wt.% Pt). LSVs at 5mV s^{-1} (a) and overpotential estimated at -10 mA cm^{-2} (b) for the 0.6 mg cm^{-2} electrocatalyst loadings on RDE rotating at 1600 rpm in N_2-saturated 1M KOH.

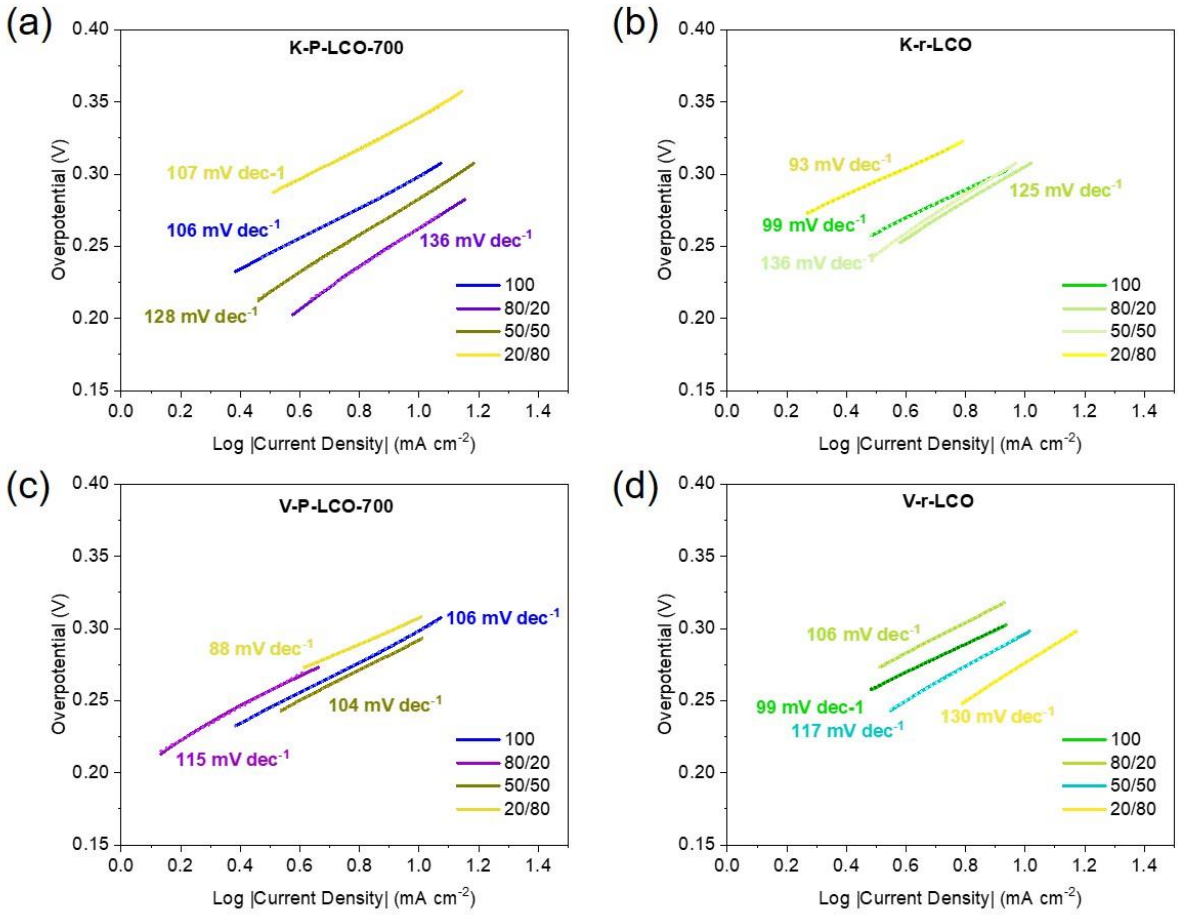

Figure S6: Tafel plots obtained for K-p-LCO-700 (a), K-r-LCO (b), V-p-LCO-700 (c) and V-r-LCO (d) with different ratios of active material and carbon back (0 to 80%).

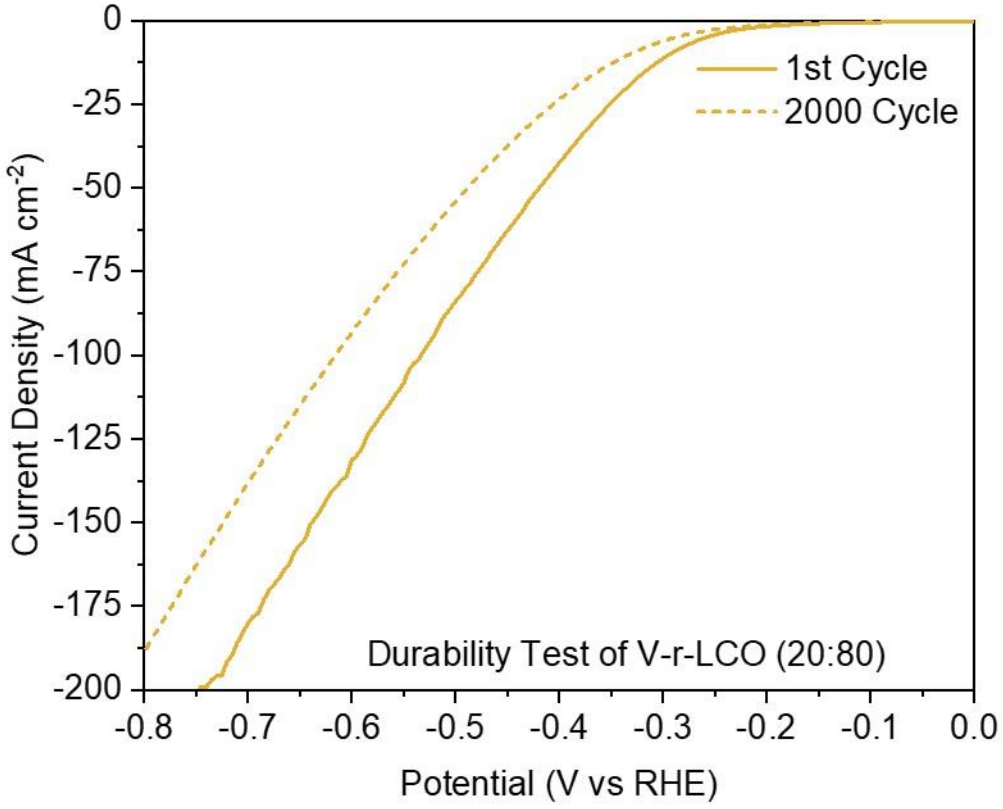

Figure S7: Accelerated Stability Test over the sample V-r-LCO (20/80) acquired by applying 2000 CV cycles under the stationary conditions with the electrocatalyst loading of 0.6 mg cm^{-2} loading in N_2-saturated 1M KOH. The initial and final CV were recorded at the scan rate of 5 mV s^{-1} while in between the sample was cycled at a 50 mV s^{-1} scan rate.

Table S2: Comparison of the performance with other Co-based electrocatalysts for HER

Sample	Overpotential at -10 mA cm^{-2} (mV)	Tafel Slope (mV dec^{-1})	Electrolyte	Reference
K-p-LCO-700 (80/20)	262	136	1M KOH	This Work
V-r-LCO (20/80)	273	130	1M KOH	This Work
CoS_2/MoS_2/NC-25%	215	80	0.5 M H_2SO_4	[13]
Co-NCNTs-10	204		1 M KOH	[14]
CoP@BCN-1	215	52	1M KOH	[15]
Co/N-C-700	84	128	1M KOH	[16]
Fe–Co–O/Co@NC-mNS/NF	112	96	1M KOH	[17]
Cu@Cu-Ni-Co	125	79.1	1M NaOH	[18]
Fe-Co_3O_4/NF	196	109	1M KOH	[19]
Waste LCOd	277	-	1M KOH	[20]
Co/Co_3O_4	90	44	1M KOH	[21]
CoN-Gr-2	128	67.35	1M KOH	[22]

References

1. da Silva Freitas, W., Mecheri, B., Lo Vecchio, C., Gatto, I., Baglio, V., Ficca, V.C.A., Patra, A., Placidi, E., D'Epifanio, A.: Metal-organic-framework-derived electrocatalysts for alkaline polymer electrolyte fuel cells. J Power Sources. 550, 232135 (2022). https://doi.org/10.1016/J.JPOWSOUR.2022.232135

2. Wei, W., Chen, W., Ivey, D.G.: Rock salt-spinel structural transformation in anodically electrodeposited Mn-Co-O nanocrystals. Chemistry of Materials. 20, 1941–1947 (2008). https://doi.org/10.1021/cm703464p

3. Zhu, J., Gao, Q.: Mesoporous MCo2O4 (M = Cu, Mn and Ni) spinels: Structural replication, characterization and catalytic application in CO oxidation. Microporous and Mesoporous Materials. 124, 144–152 (2009). https://doi.org/10.1016/J.MICROMESO.2009.05.003

4. Biesinger, M.C., Payne, B.P., Grosvenor, A.P., Lau, L.W.M., Gerson, A.R., Smart, R.S.C.: Resolving surface chemical states in XPS analysis of first row transition metals, oxides and hydroxides: Cr, Mn, Fe, Co and Ni. Appl Surf Sci. 257, 2717–2730 (2011). https://doi.org/10.1016/J.APSUSC.2010.10.051

5. Ricciardi, B., Mecheri, B., da Silva Freitas, W., Ficca, V.C.A., Placidi, E., Gatto, I., Carbone, A., Capasso, A., D'Epifanio, A.: Porous Iron-Nitrogen-Carbon Electrocatalysts for Anion Exchange Membrane Fuel Cells (AEMFC). ChemElectroChem. 10, e202201115 (2023). https://doi.org/10.1002/CELC.202201115

6. Ricciardi, B., da Silva Freitas, W., Mecheri, B., Nisa, K.U., Montero, J., Ficca, V.C.A., Placidi, E., Alegre, C., D'Epifanio, A.: Hierarchical porous Fe/Ni-based bifunctional oxygen electrocatalysts for rechargeable zinc-air batteries. Carbon N Y. 219, 118781 (2024). https://doi.org/10.1016/J.CARBON.2023.118781

7. Bennet, J., Tholkappiyan, R., Vishista, K., Jaya, N.V., Hamed, F.: Attestation in self-propagating combustion approach of spinel AFe2O4 (A = Co, Mg and Mn) complexes bearing mixed oxidation states: Magnetostructural properties. Appl Surf Sci. 383, 113–125 (2016). https://doi.org/10.1016/J.APSUSC.2016.04.177

8. Marasi, M., Panunzi, A.P., Duranti, L., Lisi, N., Di Bartolomeo, E.: Enhancing Oxygen Reduction Activity and Structural Stability of La0.6Sr0.4FeO3-δby 1 mol % Pt and Ru B-Site Doping for Application in All-Perovskite IT-SOFCs. ACS Appl Energy Mater. 5, 2918–2928 (2022). https://doi.org/10.1021/acsaem.1c03613

9. Draz, U., Bartolomeo, E. Di, Panunzi, A.P., Laverdura, U.P., Lisi, N., Chierchia, R., Duranti, L.: Copper-Enhanced CO2 Electroreduction in SOECs. ACS Appl Mater Interfaces. 16, 8842–8852 (2024). https://doi.org/10.1021/acsami.3c17766

10. Zuccante, G., Muhyuddin, M., Ficca, V.C.A., Placidi, E., Acciarri, M., Lamanna, N., Franzetti, A., Zoia, L., Bellini, M., Berretti, E., Lavacchi, A., Santoro, C.: Transforming Cigarette Wastes into Oxygen Reduction Reaction Electrocatalyst: Does Each Component Behave Differently? An Experimental Evaluation. ChemElectroChem. 11, e202300725 (2024). https://doi.org/10.1002/CELC.202300725

11. Rahimihaghighi, M., Gigli, M., Ficca, V.C.A., Placidi, E., Sgarzi, M., Crestini, C.: Lignin-Derived Sustainable Nano-Platforms: A Multifunctional Solution for an Efficient Dye Removal. ChemSusChem. 17, e202400841 (2024). https://doi.org/10.1002/CSSC.202400841

12. Jeong, S., Kim, J., Mun, J.: Self-Generated Coating of LiCoO 2 by Washing and Heat Treatment without Coating Precursors . J Electrochem Soc. 166, A5038–A5044 (2019). https://doi.org/10.1149/2.0071903JES/XML

13. Ji, K., Matras-Postolek, K., Shi, R., Chen, L., Che, Q., Wang, J., Yue, Y., Yang, P.: MoS2/CoS2 heterostructures embedded in N-doped carbon nanosheets towards enhanced hydrogen evolution reaction. J Alloys Compd. 891, 161962 (2022). https://doi.org/10.1016/j.jallcom.2021.161962

14. Zhang, S., Xiao, X., Lv, T., Lv, X., Liu, B., Wei, W., Liu, J.: Cobalt encapsulated N-doped defect-rich carbon nanotube as pH universal hydrogen evolution electrocatalyst. Appl Surf Sci. 446, 10–17 (2018). https://doi.org/10.1016/j.apsusc.2018.03.033

15. Tabassum, H., Guo, W., Meng, W., Mahmood, A., Zhao, R., Wang, Q., Zou, R.: Metal–Organic Frameworks Derived Cobalt Phosphide Architecture Encapsulated into B/N Co-Doped Graphene Nanotubes for All pH Value Electrochemical Hydrogen Evolution. Adv Energy Mater. 7, (2017). https://doi.org/10.1002/aenm.201601671

16. Li, C.-F., Zhao, J.-W., Xie, L., Wu, J.-Q., Li, G.-R.: Water Adsorption and Dissociation Promoted by Co*-/N-C*-Biactive Sites of Metallic Co/N-Doped Carbon Hybrids for Efficient Hydrogen Evolution. Appl Catal B. 282, 119463 (2021). https://doi.org/10.1016/j.apcatb.2020.119463

17. Singh, T.I., Rajeshkhanna, G., Pan, U.N., Kshetri, T., Lin, H., Kim, N.H., Lee, J.H.: Alkaline Water Splitting Enhancement by MOF-Derived Fe–Co–Oxide/Co@NC-mNS Heterostructure: Boosting OER and HER through Defect Engineering and In Situ Oxidation. Small. 17, (2021). https://doi.org/10.1002/smll.202101312

18. Younus, H.A., Al Hinai, M., Al Abri, M., Al-Hajri, R.: Hierarchical Core-Shell Cu@Cu-Ni-Co Alloy Electrocatalyst for Efficient Hydrogen Evolution in Alkaline Media. Energies (Basel). 18, 1515 (2025). https://doi.org/10.3390/en18061515

19. Su, Y., Liu, B., Shi, Z., Yan, M., Ma, T.: A Dual-Function Fe-Doped Co3O4 Nanosheet Array for Efficient OER and HER in an Alkaline Medium. Molecules. 30, 1046 (2025). https://doi.org/10.3390/molecules30051046

20. Mirshokraee, S.A., Muhyuddin, M., Morina, R., Poggini, L., Berretti, E., Bellini, M., Lavacchi, A., Ferrara, C., Santoro, C.: Upcycling of waste lithium-cobalt-oxide from spent batteries into electrocatalysts for hydrogen evolution reaction and oxygen reduction reaction: A strategy to turn the trash into treasure. J Power Sources. 557, 232571 (2023). https://doi.org/10.1016/j.jpowsour.2022.232571

21. Yan, X., Tian, L., He, M., Chen, X.: Three-Dimensional Crystalline/Amorphous Co/Co $_3$ O $_4$ Core/Shell Nanosheets as Efficient Electrocatalysts for the Hydrogen Evolution Reaction. Nano Lett. 15, 6015–6021 (2015). https://doi.org/10.1021/acs.nanolett.5b02205

22. Liu, T., Cai, S., Zhao, G., Gao, Z., Liu, S., Li, H., Chen, L., Li, M., Yang, X., Guo, H.: Recycling valuable cobalt from spent lithium ion batteries for controllably designing a novel sea-urchin-like cobalt nitride-graphene hybrid catalyst: Towards efficient overall water splitting. Journal of Energy Chemistry. 62, 440–450 (2021). https://doi.org/10.1016/j.jechem.2021.03.052